

## Analysis of the Confinement Loss and Birefringence of Index-Guided Photonic Crystal Fibres (PCF) in the Visible Spectrum

Mukesh Kumar<sup>1</sup>, Manoj Kumar<sup>2</sup>

<sup>1</sup>M.Tech.Scholar, Department of Electronics & Communication Engineering, BRCM-CET, Bahal, INDIA

<sup>2</sup>Assistant Professor, Department of Electronics & Communication Engineering, BRCM-CET, Bahal, INDIA

### ABSTRACT

This paper presents a comparative study of confinement ability of two 4-ring hexagonal lattice index-guided PCFs with different air-hole spacing (pitch) in the visible spectrum. From analysis and comparison of the two optimized PCF structures, it can be investigated that the confinement loss is very low in the structure designed with  $d/\Lambda = 0.5$  and  $\Lambda = 1.4\mu\text{m}$ , where the light is single mode and confined in the core for the visible region (400-700)nm. A low confinement loss and low birefringence of the order of  $10^{-3}$  and  $10^{-4}$  respectively are obtained for this PCF. Also the effective area is found to be nearly  $2-3\mu\text{m}^2$  and nonlinearity coefficient as  $198-82\text{km}^{-1}\text{w}^{-1}$ , extremely high confinement ability in the visible range and non-linearity makes it promising for non-linear and sensing applications.

By doing comparative study we will try to show that the structure with higher pitch value ( $1.4\mu\text{m}$ ) has got very low confinement loss of the order of  $10^{-3}$ . The numerical simulation result of proposed PCF will indicate that it has high power handling capability up to  $0.34\text{Gw}/\text{cm}^2$  and a low Birefringence of the order of  $10^{-4}$ . This PCF has small effective area about  $2-3\mu\text{m}^2$  in the visible spectrum and corresponding non-linearity co-efficient are obtained as  $198-82\text{km}^{-1}\text{w}^{-1}$ .

**Keywords**-- Photonic crystal fiber(PCF), Confinement loss, effective refractive index, finite element method.

### I. INTRODUCTION

Photonic crystal fibres are innovative technology based on the specific behavior of light in periodic

dielectric structures. Basic properties of light guidance in PCFs can be understood but for deeper insight, advanced numerical simulations must be performed. Due to band-gaps, light guidance in media with lower refractive index or even in the hollow core is possible. PCFs have numerous interesting features which can be tailored only by geometry of transverse microstructure. These features are being intensively investigated and first applications of PCFs are emerging. The two main designs of PCFs are solid-core PCF, which can be designed as single mode fibre all wavelengths and hollow-core PCF, in which light is guided due to photonic band-gap in the cladding. PCFs are promising technology for high power fibre lasers and high power light transmission. In telecommunications, PCFs can be used for auxiliary devices, whilst for usual waveguides, the attenuation at telecom frequencies must still be reduced and the cost effectiveness on the market must be achieved.

The design of There are several parameters to control: air hole shape and diameter, refractive index of the glass, type of lattice and distance between hole to hole that is lattice pitch. Autonomy of design allows one to obtain endlessly single mode fibres, which are single mode in all optical range and a cut-off wavelength does not exist. By manipulating the structure it is probable to design desired dispersion properties of the fibre. PCFs having zero, low, or anomalous dispersion at visible wavelengths can be designed and fabricated. In this paper, we have tried to get the effective modal index of hexagonal PCF considering different lattice pitch using OPTI FDTD.

## II. BIREFRINGENCE & CONFINEMENT LOSS

Birefringence is the optical property of a material having a refractive index that depends on the polarization and propagation direction of light. These optically anisotropic materials are said to be birefringent (or birefractive). The birefringence is often quantified as the maximum difference between refractive indices exhibited by the material. Crystals with asymmetric crystal structures are often birefringent, as well as plastics under mechanical stress. Birefringence is responsible for the phenomenon of double refraction whereby a ray of light, when incident upon a birefringent material, is split by polarization into two rays taking slightly different paths. This effect was first described by the Danish scientist Rasmus Bartholin in 1669, who observed it in calcite, a crystal having one of the strongest birefringence. However it wasn't until the 19th century that Augustin-Jean Fresnel correctly described the phenomenon in terms of polarization, understanding light as a wave with field components in transverse polarizations (perpendicular to the direction of the wave vector). The simplest (and most common) type of birefringence is that of materials with uniaxial anisotropy. That is, the structure of the material is such that it has an axis of symmetry with all perpendicular directions optically equivalent. This axis is known as the optic axis of the material, and components of light with linear polarizations parallel and perpendicular to it have unequal indices of refraction, denoted  $n_e$  and  $n_o$ , respectively, where the subscripts stand for extraordinary and ordinary. The names reflect the fact that, if unpolarized light enters the material at some angle of incidence, the component of the incident radiation whose polarization is perpendicular to the optic axis will be refracted according to the standard law of refraction for a material of refractive index  $n_o$ , while the other polarization component, the so-called extraordinary ray will refract at a different angle determined by the angle of incidence, the orientation of the optic axis, and the birefringence. What's more, the extraordinary ray is an inhomogeneous wave whose power flow (given by the Poynting vector) is not exactly parallel to the wave vector. This causes a shift in that beam, even when launched at normal incidence, that is popularly observed using a crystal of calcite as photographed above. Rotating the calcite crystal will cause one of the two images that of the extraordinary ray, to rotate slightly around that of the ordinary ray which remains fixed. When the light propagates either along or orthogonal to the optic axis, such a lateral shift does not occur. In the first case, both polarizations see the same effective refractive index, so there is no extraordinary ray. In the second case the extraordinary ray propagates at a different phase velocity (corresponding to  $n_e$ ) but is not an inhomogeneous wave.

Confinement losses in PCFs occur for a number of reasons, such as intrinsic material absorption loss, structural imperfection loss, Rayleigh scattering loss, confinement loss, and so on. Fabrication-related losses can be reduced by carefully optimizing the fabrication process. Confinement loss is an additional form of loss that occurs in single-material fibers [13]. The  $SiO_2$  materials don't have an imaginary component because they are not absorbing. PCFs are usually made from pure silica, and so the guided modes are inherently leaky because the core index is the same as the index of the outer cladding without air-holes. Because of the finite transverse extent of the confining structure, the effective index is a complex value; its imaginary part  $Im(n_{eff})$  is related to losses  $L$  (in decibels per meter) through the relation [19];

$$L = \frac{40\pi \cdot Im(n_{eff}) \times 10^6}{\lambda \cdot \ln(10)} \dots\dots\dots Eq. 1$$

This confinement loss can be reduced exponentially by increasing the number of air-holes rings that surround the solid core, and is determined by the geometry of the structure. Also, increasing the air-holes diameter results in the increasing of the air filling fraction which is calculated by the following equation in triangular lattice and consequently decreasing the loss,

$$F = \frac{\pi}{2\sqrt{3}} \left( \frac{d}{\Lambda} \right)^2 \dots\dots\dots Eq. 2$$

It is important to know how many numbers of airholes rings are required to reduce the confinement loss under the Rayleigh scattering limit for practical fabrication process.

## III. SIMULATION OF PCF IN VISIBLE SPECTRUM

In OptiFDTD, the mode solver is combined with the FDTD [10] engine so that FDTD simulation can use the modal field as input directly. In addition to this integrated mode solver, OptiFDTD also provides an independent mode solver to allow user to solve and study the mode outside of an FDTD calculation. The PCF mode solver will mainly be used as an independent mode solver. Visible spectrum is the portion of the electromagnetic spectrum that is visible to (can be detected by) the human eye. Electromagnetic in this range of wavelengths is called visible light or simply light. A typical human eye will respond to wavelengths from about 390 to 700 nm. In terms of frequency, this corresponds to a band in the vicinity of 430–790 THz. A light-adapted eye generally has its maximum sensitivity at around 555 nm (540 THz), in the green region of the optical spectrum (see: luminosity function). The spectrum does not, however, contain all the colors that the human eyes and brain can distinguish.

Unsaturated colors such as pink, or purple variations such as magenta, are absent, for example, because they can be made only by a mix of multiple wavelengths. Colors containing only one wavelength are also called pure colors. The full- vectorial finite difference method for TE mode (Xpolarization) and the TBC boundary condition is used for the simulation boundaries [12]. The various layouts designed and investigated using OPTIWAVE SYSTEM-DTD mode solver tool and graphs are plotted using Origin Pro 8 (The data analyzing and work space).

**A. Configuration-I**

The PCF layout has hexagonal lattice with circular air holes, Base material =silica (n=1.45)  
 Air hole diameter (d) = 0.75μm, Number of air hole rings = 4, Lattice constant (Λ) = 1.4 μm, Lattice type = Hexagonal, Diameter to pitch ratio (d/ Λ) = 0.5.

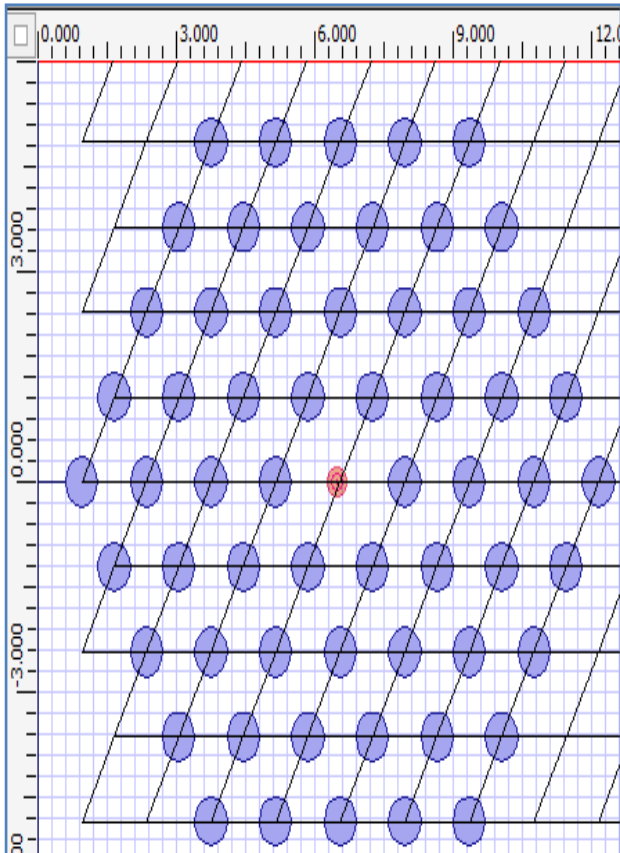


Figure 1 : PCF structure-1 layout

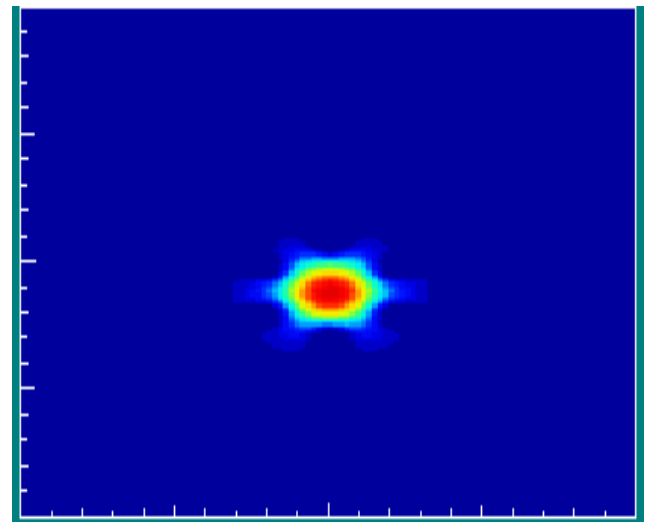


Figure 2: Field distribution at λ = 1.4

**B. Configuration-II**

The PCF layout has hexagonal lattice with circular air holes, Base material =silica (n=1.45)  
 Air hole diameter (d) = 0.6μm, Number of air hole rings = 4, Lattice constant (Λ) = 1.2μm, Lattice type = Hexagonal, Diameter to pitch ratio (d/ Λ) = 0.5.

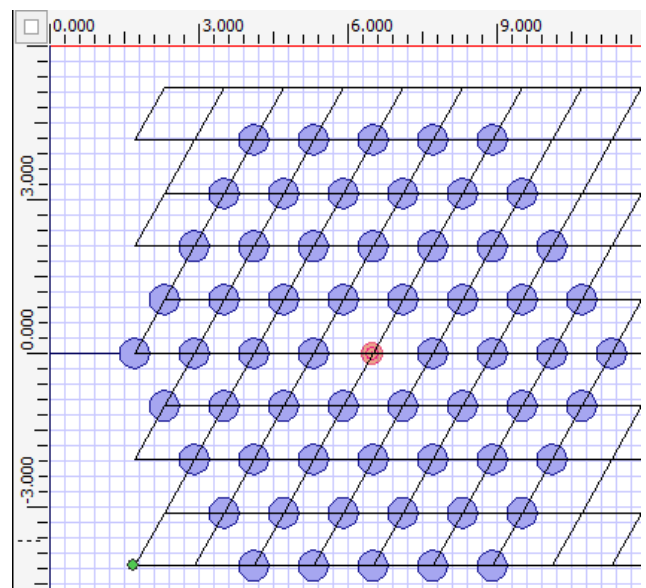


Figure 3: PCF layout Design for structure-2

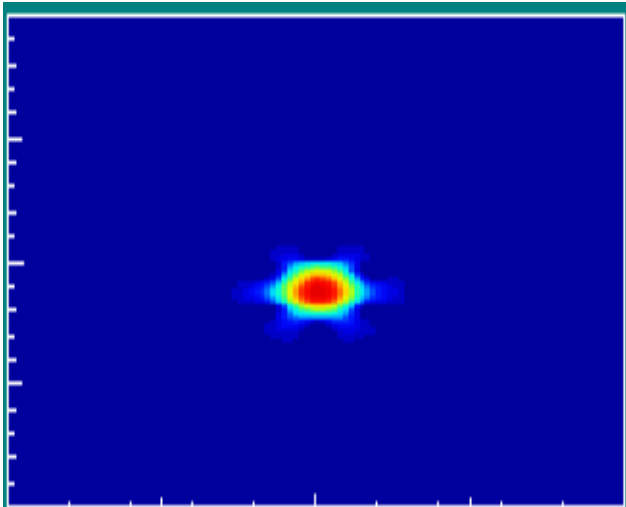


Figure 4: Field distribution at  $\lambda = 1.2$

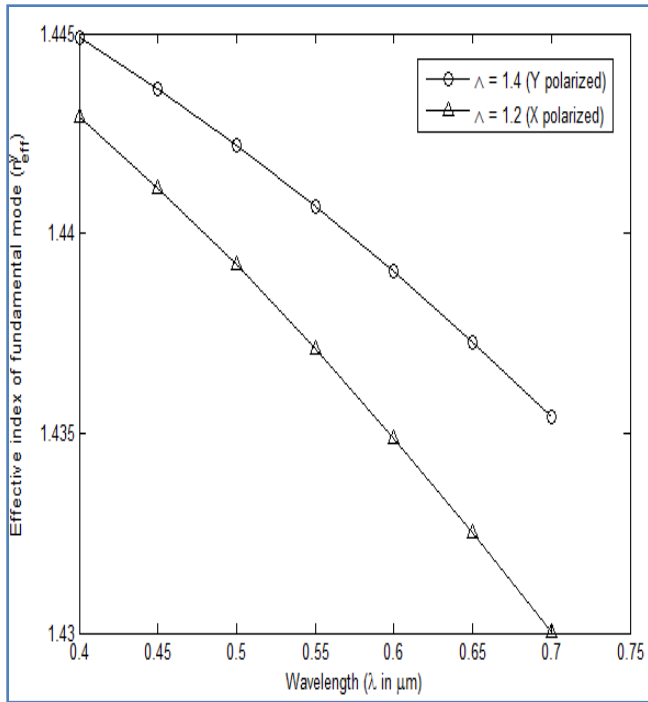


Figure 5: Effective index as a function of wavelength for the two values of pitch (1.2 and 1.4) and Y polarization

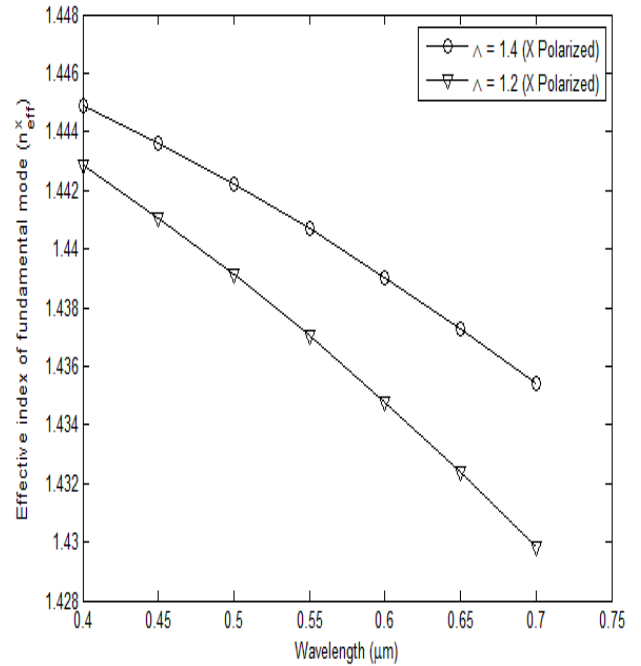


Figure 6 : Effective index as a function of wavelength for the two values of pitch (1.2 and 1.4) and X polarization.

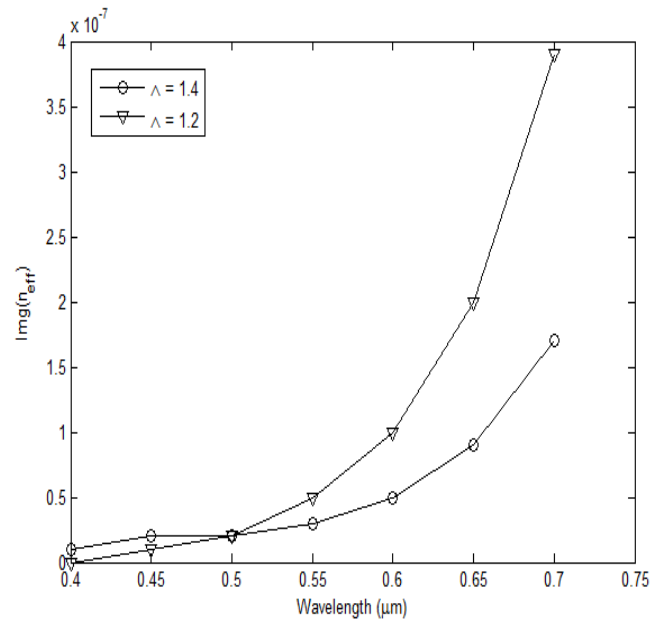


Figure 7: Imaginary part of the effective core index showing the losses in the propagation for different pitch values of the design

Confinement loss calculated on the basis of the imaginary part of the effective cladding index using the following expression of the confinement loss:

$$\text{Confinement loss (CL)} = \frac{20}{\log_e 10} \frac{2\pi}{\lambda} \text{Im}(n_{eff}) \dots \text{eq.3}$$

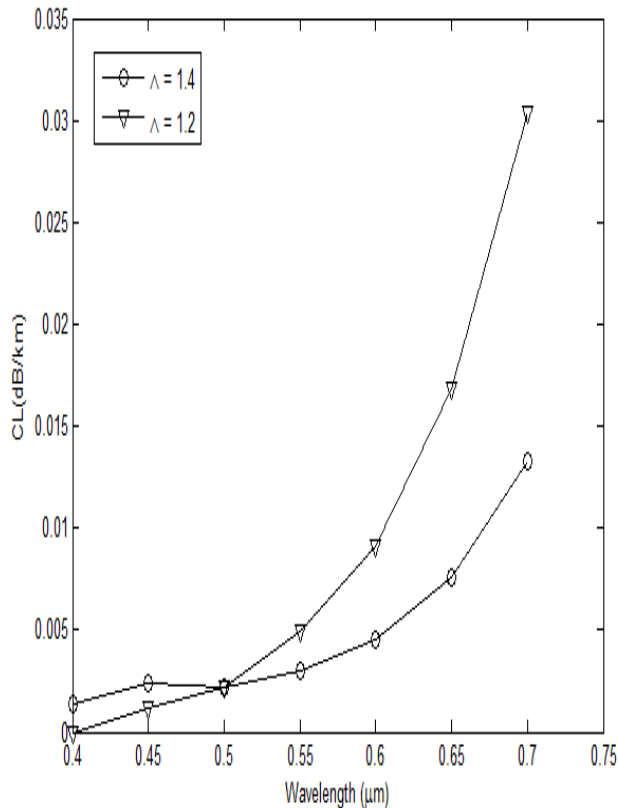


Figure 8: Confinement loss V/s wavelength

#### IV. CONCLUSION

We have proposed the design methodology of PCF for SM operation with very low confinement loss in visible range. The comparative study shows that the structure with higher pitch value ( $1.4 \mu\text{m}$ ) has got very low confinement loss of the order of  $10^{-3}$ . The numerical simulation result of proposed PCF shows that it has high power handling capability upto  $0.34 \text{Gw/cm}^2$  and a low Birefringence of the order of  $10^{-4}$ . This PCF has small effective area about  $2\text{-}3 \mu\text{m}^2$  in the visible spectrum and corresponding non-linearity coefficients are obtained as  $198\text{-}82 \text{km}^{-1} \text{w}^{-1}$ . The proposed PCF is well suitable for guiding light in visible wavelength ranges and is well suitable for the bio-sensing applications.

#### REFERENCE

- [1] S. Smolka, M. Barth, and O. Benson, "Highly Efficient Fluorescent Sensing with Hollow-core Photonic Crystal Fibers," *Opt. Express*, vol. 15, No. 20, 1 Oct 2007.
- [2] Philip Russell, "Photonic Crystal Fibers", *Applied physics Review*, SCIENCE VOL 299, 17 JANUARY 2003.
- [3] F. Poli, A. Cucinotta, S. Selleri, "Photonic Crystal Fibers, Properties and Applications," Springer series in material science 102, 2007.
- [4] C. Knight, T. A. Birks, P. S. J. St. J. Russell, and D. M. Atkin, "All-silica single-mode optical fiber with photonic crystal cladding," *Opt. Lett.*, vol. 21, pp. 1547-1549, Oct. 1996.
- [5] T. A. Birks, J. C. Knight, and P. S. J. St. J. Russell, "Endlessly single-mode photonic crystal fiber," *Opt. Lett.*, vol. 22, pp. 961-963, July 1997.
- [6] J. C. Knight, J. Broeng, T. A. Birks, and P. S. J. St. J. Russell, "Photonic band gap guidance in optical fiber," *Science*, vol. 282, pp. 1476-1478, Nov. 1998.
- [7] R. F. Cregan, B. J. Mangan, J. C. Knight, T. A. Birks, P. S. J. St. J. Russell, P. I. Roberts, and D. C. Allan, "Single-mode photonic band gap guidance of light in air," *Science*, vol. 285, pp. 1537-1539, Sept. 1999.
- [8] Villatoro, V. P. Minkovich, V. Pruneri, and G. Badenes, "Simple all-microstructured-optical-fiber interferometer built via fusion splicing," *Opt. Express*, Vol. 15, No. 4, 19 February 2007.
- [9] S. S. Mishra, Vinod K. Singh, "Designing of Index-Guiding Photonic Crystal Fiber by Finite Element Method Simulation," *Int. J. Advanced Networking and Applications* 666, Volume: 02, Issue: 03, Pages: 666-670 (2010).
- [10] Ya-Ni Zhang, "Design and optimization of high-birefringence low-loss crystal fiber with two zero-dispersion wavelengths for nonlinear effects", *APPLIED OPTICS*, Vol. 50, No. 25., 1 September 2011.
- [11] J. Knight, T. Birks, B. Mangan and P. St. James Russell, "New solutions in fiber optics," *Optics Photonics News*, vol. 13, pp. 26-30, Mar. 2002.
- [12] P. St. J. Russell, "Photonic crystal fibers," *Opt. Science*, vol. 299, pp. 358-362, Jan. 2003
- [13] J. C. Knight, J. Broeng, T. A. Birks, and P. St. J. Russell, "Photonic band gap guidance in optical fibers," *Opt Science*, vol. 282, pp. 1476-1478, Nov. 1998
- [14] J. C. Knight, J. Broeng, T. A. Birks, and P. St. J. Russell, "Photonic band gap guidance in optical fibers," *Opt Science*, vol. 282, pp. 1476-1478, Nov. 1998